

Transitions to Intermittency and Collective Behavior in Randomly Coupled Map Networks

D. Volchenkov*, S. Sequeira† and Ph. Blanchard

*Zentrum für interdisziplinäre Forschung (ZiF) and BiBoS,
University Bielefeld, Postfach 100131, D-33501, Bielefeld, Germany*

May 20, 2019

Abstract

We study the collective behavior in a random network of coupled Chaté - Manneville (CM) maps where the relevant variables are the connectivity k , coupling ε , and the governing parameter of map r . We show that for some interval of their values at least a considerable fraction of network sites display a spatio-temporal intermittency. Within the intermittency window, the system exhibits a complex collective periodic behavior. The detailed behavior crucially depends upon the topology of the random graph spanning the network. Our approach is based on the thermodynamic formalism (TD) and random graph theory.

Keywords: *coupled chaotic maps, random graphs, phase transitions, nontrivial collective behavior, spatio-temporal intermittency*

PACS codes: *05.45.+b, 05.70.Fh.*

AMS codes: *82C26, 58F11.*

Contents

1	Introduction and Motivation	2
2	The Definition of Model	4
2.1	Coupled Ensembles of the Chaté-Manneville Maps	4
2.2	Various Models of Random Networks	5
3	The Sketch of Numerical Results	6
3.1	The onset of spatio-temporal intermittency	7
3.2	The onset of non-trivial collective n -periodic behavior	7
3.3	The windows of turbulence and relaminarization	8

*dima.volchenkov@uni-bielefeld.de

†sandra@mathematik.uni-bielefeld.de

4 Probabilistic Geometrical Properties of $\mathbb{G}(N, k)$	9
4.1 The structure of in-components	9
4.2 The configuration model and subgraphs classification	10
4.3 The counting of small subgraphs and configuration	10
4.4 Hamilton Cycles and Perfect Matching	11
4.5 Sharp and coarse thresholds in RCMN	12
5 Thermodynamic Formalism for Coupled Maps Defined on the Random Networks	13
5.1 The definition of randomly coupled map networks	14
5.2 The symbolic dynamics and Gibbs states for the RCMN	15
6 Transitions to Intermittency and Collective Behavior in the RCMN	16
6.1 The equation for the free energy function	16
6.2 Transitions to the spatio-temporal intermittency and relaminarization	18
6.3 Transitions to the collective behavior in RCMN	20
6.4 The bifurcation route to collective periodic behavior in RCMN	21
7 Conclusion	21
8 Acknowledgements	22
9 Figures and Graphs	24

1 Introduction and Motivation

Partial differential equations describing continuous models and real physical systems can be discretized into a system of coupled map lattices (CML). A close attention to these systems has been drawn in virtue of studies of the generic properties of spatiotemporal chaos, [1]-[2]. In the present communication, we apply to mean-field extensions of CML. One of them is a globally coupled map lattice introduced by Kaneko in [3]. However, we consider another mean-field extension which refers to random networks.

Although just a few studies devoted to randomly coupled chaotic map networks (RCMN) have been reported by this time, it is beyond a dispute that such systems would be very reach in practical applications. To motivate the increasing interest RCMN, one has to note that most of real-world networks are of a disordered structure. In this context, the interesting observations of coupled map systems defined on the irregular structure lattices have been reported in [10] (CML's on a Serpinski gasket) and in [11] (CML's on a Cayley tree). The social networks [12], biological communities forming the food webs [13], and, moreover, the computer networks [14] to name just few of them have a plenty of random shortcuts inconsitstable with any regular

structure. In view of this, an ensemble of maps coupling at random would provide a forthright model to some of their properties. The thorough investigation of RCMN would shed a new light on the problem of spatio-temporal behavior of the discrete extended systems having infinitely many degrees of freedom.

Up to our knowledge, the randomly coupled logistic maps $f(x) = ax(1 - x)$ had been considered first in [4]. In [5], the coupled maps $f(x) = 1 - ax^2$ connected symmetrically at random had been discussed. It has been shown that both the mutual synchronization and the dynamical clustering appear in randomly coupled maps when approximately a half of potential connections are present. Nevertheless, they are different, in some aspects, from those known for the globally coupled maps.

We study the collective behavior and phase transitions in a RCMN different from those considered in [4] and [5]. We display that the entire collective behavior is a net result of interplay between the properties of local map and the probabilistic topology of relevant random graph.

In the present paper, somewhat the "statistically simplest" RCMN is considered. From one hand, the Chat -Manneville map (CM) [6] which we use as a local evolution law can be either in a "turbulent" (excited) state or in a "laminar" (inhibited) one. In the excited state, it generates a chaotic time series with Liapunov exponent $\lambda_0 = \log r > 0$, while, in the inhibited state, $\lambda_0 = 0$.

From another hand, the network topology in our model is spanned with a random graph $\mathbb{G}(N, k)$ such that each site of it has precisely k outgoing edges. The graph entropy [27], in this case, can be readily calculated as $h(\mathbb{G}(N, k)) = \log_2 k$. It is positive as $k \geq 2$, and $h(\mathbb{G}(N, k)) = 0$ as $k = 1$.

Let us note that, in the domain of coupled chaotic maps, the notion of phase transition is traditionally applied to at least two different classes of phenomena. The first class constitutes the case when a valuable fraction of nodes in the lattice becomes either excited or inhibited at some values of k , ε , and r . We shall call them either as a transition to intermittency or relaminarization. The second class refers to the appearance of n -periodic behavior within a sustained turbulent state. We shall call it as the transition to a collective behavior.

Our study confirms the general conclusions of [4] and [5] on the existence of a threshold connectivity value below which the synchronization does not occur. We also justify observations reported in [4] on that this threshold value would be reduced if a random graph configuration is changed at each time step.

Our approach is twofold. First, we develop the thermodynamic formalism (TD) for RCMN. Second, we use substantially the random graph theory invented by P. Erd s and A. R enyi [7] which has now developed into one of the grounds of discrete mathematics located at the intersection of graph theory, combinatorics, and probability theory [8], [9].

Taking in general, a coupled map ensemble with a "democratic" coupling refers to so called k -out model which cover the random directed graphs with vertices having precisely k outgoing edges and a random number of incoming links. Many of their properties are still to be studied.

Even for minimal connectivities k , they are typically connected. For fixed connectivity $k > 1$, they comprise of a large number of directed tree like chains, small directed cycles ("small" in the actual context means that the number of vertices in a cycle $m < N - 1$). If $k = 2$, a giant component including roughly $O(N^{2/3})$ vertices appears in the random graph for the first time. When $k \geq 3$, the Hamilton cycles which traverse all vertices of the network arise.

2 The Definition of Model

We commence with a brief definition of coupled systems of "minimal" Chaté-Manneville map [6].

2.1 Coupled Ensembles of the Chaté-Manneville Maps

Let $\Omega \subset \mathbb{Z}$ be the finite piece of lattice of $N \in \mathbb{N}$ sites. At each site $\omega \in \Omega$ there is a local phase space X_ω with an uncountable number of elements. The global phase space $M = \prod_{\omega \in \Omega} X_\omega$ is a direct product of local phase spaces such that a point $x \in M$ can be represented as $x = (x_\omega)$, $\omega \in \Omega$. The *coupled map lattice* is any mapping $\Phi : M \rightarrow M$ which preserves the product structure, $\Phi x = (\Phi_\omega x)_{\omega \in \Omega}$, in which $\Phi_\omega : M \rightarrow X_\omega$. The mapping, $\Phi = G \circ F$, is a composition of an independent local mapping $(Fx)_\omega = f_\omega(x_\omega)$, $f_\omega : X_\omega \rightarrow X_\omega$, and an interaction, $(Gx)_\omega = g_\omega(x)$.

We consider a coupled map lattice supplied with some boundary conditions,

$$(\Phi x)_\omega = \left[(1 - \varepsilon) \mathbf{I} + \frac{\varepsilon}{k} \mathbf{M} \right] f(x_\omega), \quad (1)$$

where $\varepsilon \in [0, 1]$ is the coupling strength parameter, $0 < k < N - 1$ is the connectivity number, \mathbf{I} is a unit matrix, and \mathbf{M} is a traceless connectivity matrix, $M_{jj} = 0$, determining the network topology. $M_{ij} = 0$ or 1 (in general, $M_{ij} \neq M_{ji}$).

As a local evolution law, we use the 1-parameter CM map, [6],

$$f(x) = \begin{cases} rx, & \text{if } 0 \leq x < 1/2 \\ r(1 - x), & \text{if } 1/2 \leq x < 1 \\ x, & \text{if } 1 \leq x \leq r/2, \end{cases} \quad (2)$$

where $r > 2$. For the above map, a laminar asymptotic state exists together with the possibility of a transient chaotic behavior, Fig. 1. The laminar state in (2) is *metastable* with respect to infinitesimal perturbations, $|f'(x)| = 1$, but is unstable under the localized perturbations of finite amplitude introduced by the coupling. In the Fig. 1, we present the diagram of CM map at $r = 3.0$. The uncoupled dynamics of (2) is chaotic as long as $f(x)$ remains in the unit interval since $r > 1$ and therefore the relevant Liapunov exponent $\lambda = \log r > 0$. Eventually, iterations escape to the line of marginally stable fixed points $x \in]1, r/2]$, where the iterations are locked on since $f(x) > 1$. The set of points that does not map into $]1, r/2]$ after $t \rightarrow \infty$ is a Cantor set with zero Lebesque measure [16]. We call a site as "excited" (or "turbulent"), while $x \in [0, 1]$ and as "inhibited" (or "laminar") if $1 < x \leq r/2$.

2.2 Various Models of Random Networks

In the present subsection, we give a brief review of random network architectures discussed in a literature in so far and explain the difference between them and the model which we study. We also provide their classification based on the relevant random graphs.

Let us note that because of causality property the coupled map systems are of concern to the *directed* random graphs. In the pioneering work [4], the connectivity \mathcal{K} is kept fixed, and the connectivity matrix $M_{i,j}$ is not necessary symmetric (if j is a neighbor of i , the reverse may not be true). This random network refers to a *uniform directed random graph*, denoted by $\mathbb{G}(N, \mathcal{K})$ defined on the vertex set $[N]$ with exactly \mathcal{K} edges. Denoting the family of all such graphs as \mathcal{G} , we obtain a uniform probability distribution to observe a particular realization $\mathbb{G}(N, \mathcal{K})$,

$$\mathbb{P}(\mathbb{G}) = \left(\binom{N}{2} \right)^{-1}, \quad \mathbb{G} \in \mathcal{G}.$$

Two models have been considered in [4]. In the first one, there is a "frozen disorder" with a fixed graph topology configuration.

In the second model, new connections are drawn at each time step. From the random graph theory, the second model is known as a random graph process $\{\mathbb{G}(N, \mathcal{K})\}_{\mathcal{K}}$ which begins at time 0 and adds new edges, one at a time. The \mathcal{K} -th stage of this Markov process can be identified with the uniform random graph $\mathbb{G}(N, \mathcal{K})$ as it evolves with \mathcal{K} growing from 0 to $\binom{N}{2}$.

In [5], the symmetric random connectivity matrix ($M_{ij} = M_{ji}$), the elements of which are either 0 (when the connection between maps i and j is absent) or 1 (if otherwise), has been considered (the loops were not allowed, $M_{ii} = 0$). The main advantage of this model is the independence of presence of edges, but the drawback is that the number of edges is not fixed, but varies according to a binomial distribution with an expectation

$$\binom{N}{2} p.$$

This model relies upon a *binomial* random directed simple symmetric graph, $\mathbb{G}(N, p)$, $0 \leq p \leq 1$.

Finally, the model of a random matrix has been studied in [24]. In this model, the connectivity matrix element, M_{ij} , equals to the number of times map i is connected to map j , i.e. the possible multiple edges and loops have been taken into account. Herewith, M_{ij} is not necessarily to be symmetric, and $\sum_i M_{ij} = k$ for any j , i.e. each map is coupled to k maps chosen randomly (it can be coupled to itself). We denote such a random directed graph as $\mathbb{G}^*(N, k)$.

In the present paper, we study such a scheme that the elements of connectivity matrix are taken to be either 0 or 1, herewith, the diagonal elements are always taken as 0, i.e. the coupling to itself is ruled out. The number of units in each row is fixed at $k \in [1, N - 1]$. Each vertex ω

in the relevant random graph has always k outgoing edges. The number of incoming edges is a random Poisson distributed variable with a mean $z = kN/(N - 1)$. We denote such a random directed graph as $\mathbb{G}(N, k)$. A random realization of $\mathbb{G}(16, 2)$ is given in the Fig. 4.

The random graphs $\mathbb{G}(N, 1)$ have been extensively studied in [25]-[26]. However, many properties of $\mathbb{G}(N, k)$ for arbitrary k are still to be studied. The nice property of such a graph is that they allow an explicit computation of the graph entropy $h(\mathbb{G}(N, k)) = \log k$, [27].

Let us note that, in the limit $N \rightarrow \infty$, the graph $\mathbb{G}(N, k)$ is asymptotically equivalent to $\mathbb{G}^*(N, k)$ considered in [24] since the both possibilities that either two sites will be connected more than once or one site will be coupled to itself are negligible. If $\binom{N}{2}p \approx k$, it is also asymptotically equivalent to $\mathbb{G}(N, p)$ (i.e., to a binomial random directed graph). However, it differs substantially from $\mathbb{G}(N, p)$ considered in [5] since we have $M_{ij} \neq M_{ji}$. The properties of $\mathbb{G}(N, k)$, in general, turn out to be quite different from those of either binomial random graphs or uniform random graphs (i.e. having the total number of edges fixed). For example, $\mathbb{G}(N, k)$ are typically sparse but connected.

3 The Sketch of Numerical Results

The previous studies performed for the logistic maps showed that the dynamical behavior in randomly coupled map networks is never sensitive to the initial conditions. Herewith, the mutual synchronization and dynamical clustering are possible in RCMN even with a significant fraction of all possible connections (almost 1/2) is absent. Sets of almost identical dynamical states form a dynamical hierarchy of "fuzzy" clusters [5].

Randomly coupled CM map networks have not been studied before. We observed the transitions to intermittency and to collective behavior in the random network of $N = 10^4$ sites. Numerical data show that increasing the lattice size does not much affect the results. As initial conditions, we used a random cell values uniformly distributed over the interval $[0, r/2]$. Some minimum number of initially excited cells is always required to reach the sustained turbulent state. To get rid of transients, we have discarded first 10^4 iterations then the typical observation time was 10^4 . Moreover, we have studied the both models of random topological configuration: Model A purports the random graph to be fixed while the maps are updating. It is, in fact, equivalent to a model of "frozen disorder" proposed first in [4]. In the Model B, the random graph is changed at each time simultaneously with the map values update.

Beforehand, let us note that there is no a big difference in behavior of RCMN for Model A and Model B. The transition phenomena occurring for the Model A at some values of parameters will also occur for the Model B, but in the case of Model B they appear to be more enhanced and well articulated.

As a natural order parameter monitoring the transition to intermittency, we used an instantaneous turbulent fraction, [22], $F_t = N_e(t)/N$ which is a ratio of the number of excited sites

$N_e(t)$ at time t over the total number of sites N and its mean value,

$$\langle F \rangle = \frac{1}{T} \sum_{t=1}^T F_t, \quad (3)$$

in which the first 10^4 iterations have not been taken into account. Eventually, we computed the return maps $F_{t+1}(F_t)$ to monitor the collective periodic behavior within a sustained turbulent state of the system.

3.1 The onset of spatio-temporal intermittency

The onset of spatio-temporal intermittency appears as a considerable fraction of turbulent sites in the network as the value of coupling parameter exceeds $\varepsilon > \varepsilon_c$ herewith, the actual value of ε_c depends on r chosen. For the first time, it occurs at $k = 2$ independently of r .

The random graph $\mathbb{G}(10^4, 2)$ consists of a set of small disjoint subgraphs of the length ($m \ll N$) and the largest connected component which includes about $O(N^{2/3})$ vertices [9]. In the Fig. 5, we have presented the mean turbulent fraction $\langle F \rangle$ versus ε for $\mathbb{G}(10^4, 2)$, for $r = 3.0$. One can see that as $\varepsilon > \varepsilon_c \approx 0.145$ the excitation occupies a significant fraction of vertices. The transition to spatio-temporal intermittency at $k = 2$ is characterized by the scaling relation $\langle F \rangle \propto (\varepsilon - \varepsilon_c)^\beta$, where the critical exponent $\beta = 0.55 \pm 0.03$ at $r = 3.0$.

It is to be noticed that the power law behavior of mean turbulent fraction for the diffusively coupled CM maps (i.e., with the regular nearest neighbor coupling) close to critical coupling ε_c has been reported in [6]. The value of critical exponent β obtained in [6], [16], [23] coincides with that found by us for the random network $\mathbb{G}(10^4, 2)$. Moreover, the evolution of $\langle F \rangle$ in $\mathbb{G}(10^4, 2)$ exhibits a "double jump" when the excitation comes over with 4615 nodes of the graph at the very onset and then the mean fraction grows up rapidly to 7384 nodes.

At $k = 3$, the Hamilton cycle which traverse all vertices in the graph appears for the first time. There is no any isolated vertex in $\mathbb{G}(10^4, 3)$. In the Fig. 6, one can see that the intermittency onset occurs at the critical value of coupling $\varepsilon_c \approx 0.161$. and reveals itself as a discontinuous jump of mean turbulent fraction from 0 to 4615 excited states. At the next evolution step, it grows up to 8256 nodes.

The abrupt jump of $\langle F \rangle$ as approaching the critical coupling has been observed for the *globally* coupled CM maps in [22]. nevertheless, there is an important difference between the behavior of RCMN induced by the graph $\mathbb{G}(10^4, 3)$ and that of the globally coupled CM maps studied in [22]. Namely, in contrast to the behavior presented in the Fig. 6, for any value of r , for the globally coupled map system, there is another critical value $\varepsilon'_c > \varepsilon_c > 1/2$ such that the mean turbulent fraction vanishes abruptly, giving rise to a relaminarization of the system and establishing a well defined window of turbulence on the range $[\varepsilon_c, \varepsilon'_c]$, [22].

3.2 The onset of non-trivial collective n -periodic behavior

In the Fig. 7 and Fig. 8, we have displayed the mean turbulent fraction $\langle F \rangle$ versus coupling

ε for the both Model A and Model B in the RCMN induced by the realizations of random graph $\mathbb{G}(10^4, 4)$. The error bars shown on the mean turbulent fraction $\langle F \rangle$ in Figs. 7 and 8 correspond to the standard deviation (the square root of variance) of the time series of the instantaneous fraction F_t at each value of ε . With increasing system size N , these fluctuations do not fade out. This phenomenon is associated to a nontrivial collective behavior commonly observed in the CML.

One can see that the error bars appear as $\varepsilon > 1/2$ and rise to the considerable "bulbs" close to $\langle F \rangle \approx 1$. These large amplitudes of the standard deviations reflect collective periodic states of the system. To be convinced, we consider the instantaneous turbulent fractions F_t and the return maps at different values of coupling ε which manifest the collective periodic behavior.

In the Fig. 9 and Fig. 10, we have presented the density distribution diagrams of values F_t at different couplings $\varepsilon \in [0, 1]$ for the RCMN induced by random graphs $\mathbb{G}(10^4, 25)$ and $\mathbb{G}(10^4, 30)$ consequently. At the first glance, Figs. 9 and 10 look like a pitchfork "bifurcation" diagram well known for unimodular maps on the interval $[0, 1]$.

The relevant return maps $F_{t+1}(F_t)$ for $\mathbb{G}(10^4, 25)$ show that before the onset of "bifurcations" (Fig. 11) the sustained turbulent state in the system is *unique*. However, for $\varepsilon = 0.53$ (Fig. 12), the instantaneous turbulent fraction displays an approximate periodic behavior. Other nontrivial collective states can be observed at different parameter values. For example, in the Fig. 13, the instantaneous turbulent fraction F_t displays the six-periodic cycling behavior exhibiting in the RCMN spanned with the random graph $\mathbb{G}(10^4, 30)$ at $\varepsilon = 0.56$ and $r = 3.0$.

3.3 The windows of turbulence and relaminarization

For connectivities $k \gg 1$, the relaminarization process starts at some $\varepsilon'_c > \varepsilon_c$. The mean turbulent fraction $\langle F \rangle$ vanishes establishing the well defined window of turbulence. This phenomenon has also been observed for the globally coupled CM maps [22].

Here, we observe the following evolution of the turbulent window as connectivity is enhanced.

In the Fig. 14, we have shown the mean turbulent fraction $\langle F \rangle$ versus ε for the RCMN induced by the random graph $\mathbb{G}(10^4, 10)$. The turbulent window is established within the interval of couplings $\varepsilon \in [0.33, 0.85]$. The backward transition to the laminar state appears as a discontinuous jump as it has place for the windows of turbulence in the globally coupled CM maps [22].

However, as connectivity exceeds 10, in contrast to that observed for the globally coupled CM maps, the mean turbulent fraction reduces gradually (see Figs. 15 and 16). Within the interval of connectivities $15 \leq k \leq 40$, close to the second critical value ε'_c , the decay of $\langle F \rangle$ is well approximated with the power law $\langle F \rangle \propto (\varepsilon'_c - \varepsilon)^{-\gamma}$ where the second critical exponents can be estimated as $\gamma = 0.117 \pm 0.003$ at $r = 3.0$. As $k > 40$, close to ε'_c , there are several windows of turbulence and laminar gaps appear at smaller scales.

Simultaneously, as connectivity is enhanced, the window of turbulence contracts and eventually shrinks to a point as $k \rightarrow 100$. In the Fig. 17, we have presented the behavior in the

RCMN induced by the random graph $\mathbb{G}(10^4, 60)$ at $r = 3.0$.

In the what following, we give the analysis of the observed behavior patterns in RCMN arising at different connectivity values k . Our approach combines the results of random graph theory and thermodynamic formalism. These two descriptions are, in some sense, complimentary and, therefore, yield the dipper insight in the entire behavior of RCMN.

4 Probabilistic Geometrical Properties of $\mathbb{G}(N, k)$

We commence with the random graph theory point of view. The reason for that is twofold. First, it allows to understand the threshold phenomena occurring in the transitions to intermittency and relaminarization displayed in the previous section (see Sec. 4.5). Second, the knowledge of local structures in a random graph and the counting of its small subgraphs let introduce a notion of *configuration* which is crucially important for the thermodynamic formalism applied to the chaotic coupled maps defined on a random graph (see Sec. 5).

The very first observations reported in [4] and [5] were that the detailed performance of dynamical clustering depends crucially on the entire architecture of the particular network. To define the particular probabilistic geometrical properties of a random graph, one has to chose the certain procedure of random graph generation, i.e. a *configuration model*. There is a number of constructive procedures asymptotically almost surely (a.a.s.) leading to $\mathbb{G}(N, k)$. In most of cases, nevertheless, these constructions do not give a uniformly distributed random graph, but one can check out that the relevant distributions are *contiguous* to a uniform one [9]. In this paper, we follow the configuration model proposed first in [8] which leads surely to a uniform distribution of graphs.

Given $N, k \in \mathbb{N}$ such that kN is even and $k \leq N - 1$. The vertex set of a graph is $\Omega = [N]$. While speaking of directed graphs, it is natural to define the "in-" and "out"-components separately for each vertex as the sets of vertices which can either be reached or reachable from a given vertex $\omega \in \Omega$. Let us arrange that the in-component $\mathcal{I}_t(\omega) \subset \Omega$ is a set of vertices which are coupled to a given vertex ω in (1) at time t . Consequently, we shall name a set of vertices to which the vertex ω is coupled in (1) at time $t + 1$ as the out-component $\mathcal{O}_t(\omega) \subset \Omega$.

4.1 The structure of in-components

If the connectivity k is fixed, the incoming degree $s_i = |\mathcal{I}_t(\omega_i)|$ of the vertex ω_i in a random graph is a random variable distributed in accordance with the Poisson distribution $\text{Po}(z) = z^n e^{-z} / n!$, in which $z = kN/(N - 1)$ is the average number of incoming links [9], [32]. With respect to the backward time direction, the properties of $\mathbb{G}(N, k)$ are equivalent to those of a uniform directed random graph $\mathbb{G}(N, kN/2)$ and are studied very well.

If k is small and independent of N , a.a.s all components of $\mathbb{G}(N, kN/2)$ are trees or unicyclic, the largest of them having $O(\log N)$ vertices. As the connectivity approaches to $k = 2$, fairly quickly, all the largest components merge into one giant component roughly $O(N^{2/3})$ vertices

(see Fig. 4). The size distribution of remaining small clusters behaves as $P_\mu \propto \mu^{-3/2} \exp(-\mu)$ [32]. Then, another jump of the size of giant component occurs from $O(N^{2/3})$ to roughly $O(N)$. This phenomenon of a "double jump" in the evolution of $\mathbb{G}(N, cN)$ was firstly discussed in [33].

Let us note that the appearance of the giant component at $k = 2$, nevertheless, does not guarantee that, first, there is no isolated vertices in the graph, and, second, each vertex can be reachable from a given one. In fact, as $k = 2$, the random graph consists of a number of small disjoint clusters of the sizes $m \ll N$.

4.2 The configuration model and subgraphs classification

We begin with a description of the appropriate configuration model. Now we study the graph following the forward traversal of edges that corresponds to the natural (forward) lapse of time. In the constructive procedure, we associate the disjoint k -element sets $\mathcal{O}_t(\omega)$ to each element $\omega \in \Omega$ such that $\mathbb{W}_t = \Omega \times \mathcal{O}_t(\omega)$. The points in \mathbb{W}_t are the outgoing tails, $|\mathbb{W}| = (kN - 1)!! = (kN)!/2^{kN/2}(kN/2)!$ Then, a configuration Θ_t is a partition of \mathbb{W}_t into $kN/2$ directed pairs which we call the outgoing edges. The natural projection $\Pi_t : \mathbb{W}_t \rightarrow \Omega$ projects each configuration Θ_t to a directed multigraph $\pi(\Theta_t)$. If $\pi(\Theta_t)$ lacks loops and multiple edges, it is $\mathbb{G}(N, k)$.

One has to note that if the latter condition on $\pi(\Theta_t)$ being a simple graph is omitted, we arrive at the model $\mathbb{G}^*(N, k)$ discussed in [24]. The crucial point concerning to $\mathbb{G}^*(N, k)$ is that it does not have a uniform distribution over all multigraphs on Ω since different multigraphs arise from different numbers of configurations (giving rise to the additional factors of $1/2$ for each loop and $1/m!$ for each edge of multiplicity m). Nevertheless, as $N \rightarrow \infty$ any property that holds a.a.s for $\mathbb{G}^*(N, k)$ also holds a.a.s for $\mathbb{G}(N, k)$.

With respect to the forward traversal of edges, the random graphs appearing in the above procedure are the k -regular directed random graphs. A cursory observation of the Fig. 4 convinces that such a graph comprises of a set of typical subgraphs. A standard ground for their classification is given by an excess [9]. A component \mathcal{H} of a graph is an ℓ -component if it has $K > 0$ vertices and $K + \ell$ edges. ℓ is the excess of \mathcal{H} . Note that for any connected component $\ell \geq -1$. $\ell = -1$ only for tree like components that is a finite sequence of edges (ω_i, ω_{i+1}) such that $\mathcal{O}_t(\omega_i) = \mathcal{I}_t(\omega_{i+1})$ for $1 \leq i \leq m - 1$, where m is a length of the path.

Each 0-component is unicyclic, i.e. a path that starts and terminates at the same vertex. Other complex ℓ -components with $\ell > 0$ contains at least two simple sub-cycles.

4.3 The counting of small subgraphs and configuration

Let $k = |\mathcal{O}_t(\omega)|$ and $N = |\Omega|$. Directly from definitions it follows that the probability to observe any given set of m disjoint directed edges on \mathbb{W} in a random configuration reads as, [9],

$$p_m = \frac{(kN - 2m - 1)!!}{(kN - 1)!!}. \quad (4)$$

Let us note that if m is fixed, this probability demonstrates a power law behavior

$$p_m \sim_{N \rightarrow \infty} (kN)^{-m}. \quad (5)$$

Otherwise,

$$p_m \sim_{kN-m \rightarrow \infty} \left(\frac{e}{N}\right)^m \left(k - \frac{2m}{N}\right)^{kN/2-m} k^{-kN/2}. \quad (6)$$

The latter relation follows from (4), the expression $(n-1)!! = \sqrt{2}n^{n/2}e^{-n/2}(1 + O(1/n))$, and the Stirling formula.

Let us count the number X_m^ℓ of various *small* ℓ -components of the length m (here, 'small' means $m \leq N-1$) appearing in $\mathbb{G}(N, k)$. Note that $X_m^{\ell > m-1} \equiv 0$, and $X_1^0 = 0$ is the number of loops. Therefore, X_2^0 is the number of simple directed two-vertex cycles, X_3^0 is the number of directed triangles, etc.

As $N \rightarrow \infty$, in a random graph, X_m^ℓ are the random variables such that their distributions converge jointly in \mathbb{R}^∞ to the Poisson distributions $\text{Po}(\lambda_k^\ell)$ where $\lambda_k^\ell = \mathbb{E}X_m^\ell$ are the expectations of X_m^ℓ [9].

The number of directed path ($\ell = -1$) of length m can be calculated readily, $\text{Pa}_m = (N)_m k^m \prod_{i=2}^m s_i \simeq N^m k^m \prod_{i=2}^m s_i$, in which $(N)_m$ is the falling factorial [31] and s_i is the incoming degree of the vertex ω_i . Remember that s_i is a random variable having a distribution contiguous to the Poisson one. Then, $\lambda_m^{(-1)} = \mathbb{E}X_m^{(-1)} = p_m \text{Pa}_m = \prod_{i=2}^m s_i \sim z^{m-1} = k^{m-1}$ as $N \rightarrow \infty$.

Analogously, for the number of simple cycles, one obtains $\lambda_m^0 = m^{-1} \prod_{i=1}^m s_i \sim_{N \rightarrow \infty} m^{-1} \times (k)^m$, in which the factor $1/m$ comes from all permutations of vertex indices within the cycle. Then, for the number of 1-component subgraphs, we arrive at $\lambda_m^1 = (m-2)^{-1} (k-1)^m \prod_{i=1}^m s_i \times \prod_{j=1}^{m-1} (s_j - 1) \sim_{N \rightarrow \infty} k^m (k-1)^m (k-2)^{m-1} / (m-2)$ and so on.

Due to properties of the Poisson distribution, one obtains the following asymptotic relation for the factorial moments (i.e. the number of ordered pairs $(X_m^\ell)_2$, triplets $(X_m^\ell)_3$, quadruplets $(X_m^\ell)_4$, etc.)

$$(X_{m_1}^\ell)_{i_1} (X_{m_2}^\ell)_{i_2} \dots (X_{m_n}^\ell)_{i_n} \longrightarrow_{N \rightarrow \infty} (\lambda_{m_1}^\ell)^{i_1} (\lambda_{m_2}^\ell)^{i_2} \dots (\lambda_{m_n}^\ell)^{i_n}. \quad (7)$$

A set of pairs $\Theta(\mathbb{G}) = \{m, X_m^\ell\}_{\ell=-1}^{m-1}$ is the *configuration* of a graph \mathbb{G} .

4.4 Hamilton Cycles and Perfect Matching

Hamilton cycles H are the directed cycles of length N . The analysis developed in the previous subsection gives for the expectation number of cycles $m = N$,

$$\mathbb{E}H_k = (N-1)! \frac{(kN-2N-1)!!}{(kN-1)!!} \cdot k^N \prod_{i=1}^N s_i \quad (8)$$

If $k = 0$ or 1 , then there is evidently no Hamilton cycles in $\mathbb{G}(N, k)$. If $k = 2$, then the equation (8) yields,

$$\mathbb{E}H_2 = \frac{(N-1)!}{(2N-1)!!} \sim_{N \rightarrow \infty} \sqrt{\frac{\pi}{N}} \longrightarrow_{N \rightarrow \infty} 0. \quad (9)$$

Hence there is also *a.a.s* no Hamilton cycles in $\mathbb{G}(N, 2)$.

As $k \geq 3$, the number of Hamilton cycles in $\mathbb{G}(N, k)$ exhibits a threshold. Namely, in

$$\mathbb{E}H_{k \geq 3} \sim_{N \rightarrow \infty} \sqrt{\frac{\pi}{2N}} \left[\frac{(k-2)^{k/2-1}}{k^{k/2-2}} \right]^N \quad (10)$$

the quantity within the square brackets is greater than 1 for any $k \geq 3$, therefore, $\mathbb{E}H_{k \geq 3} \rightarrow \infty$ as $N \rightarrow \infty$. Therefore, $\mathbb{G}(N, k)$ has lots of Hamiltonian cycles when $k \geq 3$. As a matter of fact, it means that $\mathbb{G}(N, k)$ has no isolated vertices as $k \geq 3$, i.e. there is a perfect matching which covers every vertex of the graph.

The case of $k = 4$ is of a particular interest since the number of edges $e = 2N$, i.e. the excess $\ell = N$. Here we refer to a result of [9] (see also references therein) about the contiguity of probability distributions defined on a simple sum of two Hamilton cycles $\mathbb{H}(N)$ and the random graph $\mathbb{G}(N, 4)$,

$$\mathbb{H}(N) + \mathbb{H}(N) \asymp \mathbb{G}(N, 4). \quad (11)$$

The latter statement means that as $N \rightarrow \infty$ the probability measures defined on $\mathbb{G}(N, 4)$ and on two independent Hamilton cycles $\mathbb{H}(N) + \mathbb{H}(N)$ are mutually absolutely continuous.

4.5 Sharp and coarse thresholds in RCMN

For many graph properties, the limiting probability that a random graph possesses them jumps from 0 to 1 very rapidly, with a rather small increase (or decrease) in the expected number of edges [9].

In the Sec. 3, we have encountered a number of threshold phenomena related to transitions to intermittency and backward to a laminar state. At the onset of intermittency, i.e. as $\varepsilon \rightarrow \varepsilon_c^-$ and r fixed, there is a monotone increasing property of $\mathbb{G}(N, k)$ to have an induced turbulent subgraph G which calls for a close attention. Similarly, as $\varepsilon \rightarrow \varepsilon'_c^-$, for r fixed, one can define a monotone decreasing property of having a laminar subgraph.

We define the intermittency threshold for the RCMN $\mathbb{G}(N, k)$ as following. Let us suppose that there are $F_t N$ excited cells in Ω at time t . Consider a subgraph $G \subseteq \mathbb{G}(N, k)$ such that the vertex set $[F_t N]$ of G is $[F_t N] \subseteq [N]$ and the edge set $E[G] = E[\mathbb{G}(N, k)] \cap (F_t N)^2$. We shall call G as the *induced turbulent subgraph* of the random graph $\mathbb{G}(N, k)$.

Directly from the definitions (1-2) one obtains that a site ω that is laminar at time t becomes turbulent at time $t+1$ if $x_\omega(t) \in [1, x_m(\omega; t)]$ where $x_m(\omega; t)$ is the maximum value that the laminar cell may have in order to become turbulent in the next iteration,

$$x_m(\omega; t) = \frac{1 - \varepsilon \varphi(\omega; t)}{1 - \varepsilon},$$

in which $\varphi(\omega; t) = s_\omega^{-1} \sum_{\omega' \in \mathcal{I}_t(\omega)} f(x_{\omega'}(t))$. Therefore, $P\{1 \leq x_\omega(t) < x_m(\omega; t)\}$ is the probability that ω becomes turbulent at the next time step. Consequently, $P\{x_m(\omega; t)/r < x_\omega(t) < 1 - x_m(\omega; t)/r\}$ is the probability that the cell ω being turbulent at time t becomes laminar at time $t+1$.

Let us denote a sequence of probabilities that the site ω is turbulent at time $t+1$ at different values of coupling ε as

$$\begin{aligned}\mathfrak{p}(\varepsilon) &= P\{1 \leq x_\omega(t) < x_m(\omega; t)\} \\ &\times (1 - P\{x_m(\omega; t)/r < x_\omega(t) < 1 - x_m(\omega; t)/r\}).\end{aligned}$$

Then we define a limit $\mathfrak{p}_c = \lim_{\varepsilon \rightarrow \varepsilon_c} \mathfrak{p}(\varepsilon)$. For an increasing property of having the induced turbulent subgraph $G \subseteq \mathbb{G}(N, k)$, a sequence $\mathfrak{p}(\varepsilon)$ is called a *threshold* if

$$\mathbb{P}\{G \subseteq \mathbb{G}(N, k)\} = \begin{cases} 0, & \mathfrak{p}(\varepsilon) \ll \mathfrak{p}_c \\ 1, & \mathfrak{p}(\varepsilon) \gg \mathfrak{p}_c. \end{cases} \quad (12)$$

Furthermore, \mathfrak{p}_c is called a *sharp* threshold if for every $\eta > 0$, $\mathbb{P}\{G \subseteq \mathbb{G}(N, k)\} = 0$ as $\mathfrak{p} \leq (1 - \eta)\mathfrak{p}_c$, and $\mathbb{P}\{G \subseteq \mathbb{G}(N, k)\} = 1$ as $\mathfrak{p} \geq (1 + \eta)\mathfrak{p}_c$, otherwise we shall call \mathfrak{p}_c as a *coarse* threshold.

Here we refer to a recent result [35] that graph properties that depend on containing a large subgraph have always sharp thresholds. A monotone graph property with a coarse threshold may be approximated by the property of containing at least one of a certain finite family of small graphs as a subgraph. This statement gives us a key to understanding the nature of transitions to intermittency occurring in RCMN.

Indeed, as $k = 2$, the random graph $\mathbb{G}(N, k)$ consists of merely small subgraphs. Some of them become turbulent as $\varepsilon \geq \varepsilon_c$, establishing a coarse threshold. If $k \geq 3$, the random graph $\mathbb{G}(N, k)$ is connected, moreover, it comprises of a number of Hamilton cycles, and consequently, the intermittency threshold is sharp. Otherwise, if the connectivity is around $k = 10$, the relaminarization process which starts as $\varepsilon \rightarrow \varepsilon'_c$ appears as a sharp threshold since, probably, a whole Hamilton cycle becomes laminar at once. However, for k which substantially exceeds 10, the relaminarization process comes step by step over small subgraphs establishing a coarse threshold.

We conclude this section with a note on a power law for a monotone graph property close to a threshold value, [9]. For a coarse threshold, there are $n \in \mathbb{N}$ and $\alpha \in \mathbb{R}$ such that $\mathfrak{p}(\varepsilon, t) \asymp n^{-\alpha}$. More precisely, there is a partition of $[N]$ into a finite number of sequences $[N_1], [N_2], \dots, [N_m]$ (i.e., induced subgraphs) and rational numbers $\alpha_1, \alpha_2, \dots, \alpha_m > 0$ such that $\mathfrak{p}(\varepsilon, t) \asymp n_j^{-\alpha_j}$ for $n_j \in [N_j]$, [9].

5 Thermodynamic Formalism for Coupled Maps Defined on the Random Networks

In the present section, we consider the thermodynamic formalism (TD) approach to the behavior of coupled maps defined on random networks. TD relies upon a symbolic representation for the coupled maps dynamics. The general idea of the approach is to study this representation via Gibbs states for the $(d+1)$ -dimensional system which goes back to [18] and [19].

5.1 The definition of randomly coupled map networks

Beforehand, we have to give a rigorous definition for ensembles of coupled maps defined on a random graph since nobody has done it so far. Probably, there are several possibilities to define them, however, the following one seems us most natural.

Consider a finite set $\Xi \subset \mathbb{Z}$ such that $|\Xi| = \mathcal{N} < \infty$ and $k \in \mathbb{Z}_+$, $k \leq \mathcal{N} - 1$, such that $k\mathcal{N}$ is even. Following the standard configuration model (Sec. 4.2), one associate the disjoint k -element sets $\mathcal{O}_t(v)$ to each element $v \in \Xi$. As a result, one arrives at the set of outgoing tails $\mathbb{W}_t = \Xi \times \mathcal{O}_t(v)$. A partition Θ_t of \mathbb{W}_t into $k\mathcal{N}/2$ directed pairs which we call the outgoing edges. Then the natural projection $\pi(\Theta_t(\mathbb{G}))$ is a simple random graph $\mathbb{G}(\mathcal{N}, k)$.

At each node $\varpi \in \Xi$, we define a local phase space X_ϖ with an uncountable number of elements. The global phase space $M_{\mathbb{G}(\mathcal{N}, k)} = \prod_{\varpi \in \Xi} X_\varpi$ is a direct product of local phase spaces such that a point $x \in M_{\mathbb{G}(\mathcal{N}, k)}$ can be represented as $x = (x_\varpi)$, $\varpi \in \Xi$.

Let us now suppose that there is a subset $\Omega \subset \Xi$ such that $|\Omega| = N \ll \mathcal{N}$. Consider a subgraph $\mathbb{G}(N, k) \subset \mathbb{G}(\mathcal{N}, k)$ such that the edge set $E[\mathbb{G}(N, k)] = E[\mathbb{G}(\mathcal{N}, k)] \cap \Omega^2$. Then $\mathbb{G}(N, k)$ is a random graph induced by Ω . For each $\omega \in \Omega$, we denote the local phase space $X_\omega \subseteq X_\varpi$ and the global phase space $M_{\mathbb{G}(N, k)} = \prod_{\omega \in \Omega} X_\omega$ such that $M_{\mathbb{G}(N, k)} \subseteq M_{\mathbb{G}(\mathcal{N}, k)}$. In the what following, we denote $M_{\mathbb{G}(N, k)}$ simply as $M_{\mathbb{G}}$. Now we push $\mathcal{N} \rightarrow \infty$.

The *randomly coupled map network* (RCMN) defined on the random graph $\mathbb{G}(N, k)$ is a mapping $\Phi_{\mathbb{G}} : M_{\mathbb{G}} \rightarrow M_{\mathbb{G}}$ which preserves the product structure, $\Phi_{\mathbb{G}}x = (\Phi_\omega x)_{\omega \in \Omega}$, in which $\Phi_\omega : M_{\mathbb{G}} \rightarrow X_\omega$

As usual, the mapping $\Phi_{\mathbb{G}} = C \circ F$, can be considered as a composition of the local mapping $(Fx)_\omega = f_\omega(x_\omega)$ which is independent from the graph topology, $f_\omega : X_\omega \rightarrow X_\omega$, and the interaction $(C_{\mathbb{G}}x)_\omega = g_\omega^{\mathbb{G}}(x)$.

In the framework of thermodynamic formalism, we seek for a symbolic representation for the dynamic of the coupled map system $(\Phi_{\mathbb{G}}x)_\omega$, $\omega \in \Omega$ on the cylinder $\mathbb{L} = \Omega \times \mathbb{Z}_+$ where $\Omega \subset \Xi$. In concern to the above definition, two models can be considered.

Model A. This is the model of "frozen disorder" proposed first in [4], there the configuration $\Theta(\mathbb{G})$ is kept as fixed while the map Φ is iterating.

Model B. There the configuration $\Theta_t(\mathbb{G})$ is changed at each time step simultaneously to map updating.

Let us note that from the definition of RCMN given above, in the limit $\mathcal{N} \rightarrow \infty$, both Model A and Model B are indeed not very different. The numbers of small subgraphs $X_m^\ell(\mathcal{N})$ in the entire random graph $\mathbb{G}(\mathcal{N}, k)$ are random variables fluctuating around their expectation values λ_m^ℓ . Let us define a discrete time *random graph process* $\{\mathbb{G}(\mathcal{N}, k)\}_{\mathcal{N}}$ which describes the growing of the entire random graph $\mathbb{G}(\mathcal{N}, k)$ as $\mathcal{N} \rightarrow \infty$. This is obviously a Markov process with time running through the discrete set $\{0, 1, \dots, k\mathcal{N}/2\}$. Hence, one has $t = O(\mathcal{N})$ as $\mathcal{N} \rightarrow \infty$.

Now let us return to $\mathbb{G}(N, k)$ which is a small subgraph of $\mathbb{G}(\mathcal{N}, k)$ induced by $\Omega \subset \Xi$. The configuration of $\mathbb{G}(N, k)$ also varies as \mathcal{N} grows. The numbers of small subgraphs $X_m^\ell(\mathcal{N}, N) \simeq$

$X_m^\ell(t, N)$ are the Poisson distributed random variables (since $\mathbb{E}(X_m^\ell)_k = (\lambda_m^\ell)^k$) such that $X_m^\ell(t, N) \rightarrow \lambda_m^\ell$ as $t \rightarrow \infty$ and $N \rightarrow \infty$. Therefore, even in the model of "frozen disorder" Model A, the actual configurations would change at each time step.

5.2 The symbolic dynamics and Gibbs states for the RCMN

Given the configuration of the entire random graph $\Theta_{\mathcal{N}} = \pi^{-1}(\mathbb{G}(\mathcal{N}, k))$, a symbolic dynamics provided it exists is defined as a direct product $\mathcal{T} = \pi^{-1} \otimes T$, where T is a semi-conjugacy (since, in principle, there would be no inverse map on the partition boundaries) to the map Φ on $M_{\mathbb{G}}$ from a subshift σ on a symbolic configuration space M_Φ^s :

$$\forall \xi \in M_\Phi^s, \quad T(\sigma\xi) = \Phi T(\xi), \quad (13)$$

and π^{-1} is conjugated to a subshift τ on a random graph configuration space \mathbb{W} ,

$$\pi^{-1}(\tau\Theta_{\mathcal{N}}) = \pi^{-1}(\Theta_{\mathcal{N}+1}). \quad (14)$$

Relations (13-14) purport a Markov partition $\mathcal{V}_{\xi, \Theta}$ to be defined with an index set $M_{\mathbb{G}}^s = A^s$ for a finite alphabet A . The simplest possible alphabet would comprise just of two letters, $A = \{0, 1\}$, indicating either "excited" or "inhibited" state.

As a result, to any spatio-temporal configuration $x \in M_{\mathbb{G}} : x = (x_\varpi), \varpi \in \Xi$, a symbolic code $\xi = (\xi_t), t \in \mathbb{Z}_+$ is assigned, and $M_{\Phi, \mathbb{G}}^s$ is the set of all such codes.

The thermodynamic formalism comes about by asking for a conditional probability distribution on symbolic configurations defined on a cylinder $\mathbb{L} = \Omega \times \mathbb{Z}_+$, $\Omega \subset \Xi$, given a symbolic configuration on the complement $\mathbb{L}^c = \Omega^c \times \mathbb{Z}_+$, $\Omega^c = \Xi \setminus \Omega$. On the uniformly hyperbolic subsets $K \subseteq M_{\mathbb{G}}$ these conditional probabilities are given by the Gibbs states,

$$P(\xi_{\mathbb{L}} | \xi_{\mathbb{L}^c}) = Z^{-1} \exp[-\mathcal{F}_{\mathbb{L}}(\xi)], \quad (15)$$

where $\mathcal{F}_{\mathbb{L}}(\xi)$, $(\xi_t)_\omega \in M_{\Phi, \mathbb{G}}^s$, $(\omega, t) \in \mathbb{L}$ is a part of the potential

$$\mathcal{F}(\xi, \Theta) = \sum_{t \in \mathbb{Z}_+} \log |\det[D^{(u)}\Phi](\mathcal{T}(\sigma^t \xi, \tau^t \Theta)_{(\varpi, t)})| \quad (16)$$

which plays the role of a Hamiltonian in the statistical mechanics. The Jacobian matrix $[D^{(u)}\Phi]$ is restricted to a unstable subspace which is the whole tangent space $TM_{\mathbb{G}}$ for expanding maps, $N \rightarrow \infty$. We shall drop the index (u) in the sequel.

The normalization factor Z in (15) is a partition function,

$$Z = \sum_{\eta \in M_{\Phi, \mathbb{G}}^s} \exp[-\beta \mathcal{F}(\eta)] \quad (17)$$

where the sum in (17) is performed over all configurations $\eta \in M_{\Phi, \mathbb{G}}^s$ which coincide with ξ on \mathbb{L} .

Although, in general, a possibility to introduce the thermodynamic formalism defined as (15-17) for a coupled map lattice at any dimension and for any values of the coupling strength $\varepsilon > 0$ is questionable, nevertheless, for a 1D piece-wise linear map it is indeed always possible, [20].

6 Transitions to Intermittency and Collective Behavior in the RCMN

All information on transitions to intermittency and collective behavior in the RCMN is included in the Gibbs potential \mathcal{F} (16). For statistical mechanics, it is somewhat unusual because even in the uncoupled case it has non-trivial interactions in the time direction [29], [30]. Nevertheless, a formal analogy between transitions to spatio-temporal intermittency observed in the RCMN and phase transitions in uniaxial ferromagnetic can be found.

For the coupled map system (1-2), the potential \mathcal{F} is a function of three external parameters, $\{\varepsilon, r, k\}$. The hyperbolicity of phase space means a positivity of all Liapunov exponents in the spectrum, $\lambda_n > 0$. From direct numerical simulations, it is known, [21], that the number of positive Liapunov exponents for extended chaotic systems scales like the lattice size, $N_{\lambda_n > 0} \sim N$. This means that in the extended limit $N \rightarrow \infty$ the instantaneous turbulent fraction $F_t = N_{\mathcal{T}}(t)/N$ is a natural order parameter monitoring the transition to intermittency in a coupled chaotic map system.

Since the matrix element of $[D\Phi]$ in (16) relevant to a site ϖ being in the turbulent state is proportional to r , the instantaneous turbulent fraction can be simply counted as

$$F_t = -\frac{\partial \mathcal{F}(r, \varepsilon, k)}{\partial r}. \quad (18)$$

The analogy with the uniaxial ferromagnetic is following. Let us assign the turbulent state to a "spin up" configuration and the laminar state to a "spin down". Then F_t is a spontaneous magnetization in the ferromagnetic with interaction Hamiltonian (16). The mean turbulent fraction,

$$\langle F \rangle = \frac{\partial \log Z}{\partial r}, \quad (19)$$

in which Z is the partition function (17), is equivalent to the magnetization in ferromagnetic.

Continuing this analogy, one can introduce the Gibbs free energy function \mathcal{U} for the system of coupled chaotic maps. Let us define a finite piece $\mathbb{L}_{\mathcal{N}} \subset \mathbb{L}$ of the cylinder $\mathbb{L} = \Omega \times \mathbb{Z}_+$ having a volume $\mathbb{V}_{\mathcal{N}} = N \cdot c\mathcal{N}$ where $c < \infty$. One can introduce a restriction $\mathcal{F}_{\mathbb{L}_{\mathcal{N}}}$ of the potential $\mathcal{F}_{\mathbb{L}}$ on the finite cylinder $\mathbb{L}_{\mathcal{N}}$. Then the free energy is $\mathcal{U} = \lim_{\mathcal{N} \rightarrow \infty} \mathcal{F}_{\mathcal{N}}/\mathbb{V}_{\mathcal{N}}$.

6.1 The equation for the free energy function

Following [29], [30], and [17], we now apply a simple transformation to (16). We use the standard relation $\log \det = \text{Tr} \log$ which gives us the following expression for the Gibbs potential:

$$\mathcal{F}_{\mathbb{L}}(\xi|_{\mathbb{L}}, \Theta) = \sum_{t \in \mathbb{Z}_+} \text{Tr} (\log |[D\Phi]|)_{\omega, \omega} (\mathcal{T}(\sigma^t \xi, \tau^t \Theta)_{(\omega, t)}), \quad (\omega, t) \in \mathbb{L}. \quad (20)$$

Since the local map (2) is 1D, then $\log D\Phi_{\omega}$ can be defined to be just the number $\log |D\Phi_{\omega}|$. The notation $(\log |[D\Phi]|)_{\omega, \omega}$ denotes the diagonal block corresponding to site $\omega \in \Omega$. The trace

is summed over the whole induced subgraph $\mathbb{G}(N, k) \subset \mathbb{G}(\mathcal{N}, k)$ and is independent of any choices.

Returning to map (1-2), one can proceed further with the potential (20). The Jacobian matrix in (20) can be written in the following form $[D\Phi] = \mathbb{U}(\mathbb{I} - \mathbb{U}^{-1}\mathbb{C})$ where \mathbb{U} is a contribution coming from the *uncoupled* maps (i.e., the diagonal part of $[D\Phi]$), and \mathbb{C} is that of coupling. Then we expand $\text{Tr} \log |[D\Phi]| = \text{Tr} \log |\mathbb{U}| - \sum_{s>0} \text{Tr} [(\mathbb{U}^{-1}\mathbb{C})^s/s]$.

The entries $\log |U_\omega|$ can take two different values depending on whether site ω is laminar or turbulent: $\log |U_\omega| = \log(1 - \varepsilon)$ if $1 \leq x_\omega \leq r/2$, otherwise, $\log |U_\omega| = \log(1 - \varepsilon) + \log r$, if $0 \leq x_\omega < 1$. Suppose that there are NF_t turbulent sites in the graph $\mathbb{G}(N, k)$ induced by Ω at time t . Therefore, $\text{Tr}(\log |\mathbb{U}_\omega|)_{(\omega, \omega)} = N \log(1 - \varepsilon) + NF_t \lambda_0$, where $\lambda_0 = \log r$ is the Liapunov exponent of the uncoupled, solitary map (2).

The series $\sum_{s>0} (\mathbb{U}^{-1}\mathbb{C})^s/s$ is of careful consideration. It is easy to check that

$$\mathbb{U}^{-1}\mathbb{C} = \frac{\varepsilon}{k(1 - \varepsilon)} \mathbb{A}_{\omega\omega'}, \quad (21)$$

in which $\mathbb{A}_{\omega\omega'}$ is the 'weighted' adjacency matrix of the random graph $\mathbb{G}(N, k)$ such that

$$\mathbb{A}_{\omega\omega'} = \begin{cases} 0, & \omega \text{ and } \omega' \text{ are not coupled,} \\ 1, & \omega \text{ and } \omega' \text{ are in the same state,} \\ r, & \omega \text{ is turbulent, } \omega' \text{ is laminar,} \\ 1/r & \omega \text{ is laminar, } \omega' \text{ is turbulent.} \end{cases} \quad (22)$$

The matrix $\mathbb{A}_{\omega\omega'}$ contains data of both topological as well as dynamical configurations of the coupled map system defined on $\mathbb{G}(N, k)$. We denote the adjacency matrix of the graph $\mathbb{G}(N, k)$ as \mathbf{A} with entries $A_{ij} = 0$ or 1 .

The number of cycles in $\mathbb{G}(N, k)$ is of crucial importance. Let us recall that $\text{Tr}(\mathbf{A}^s) = X_s^0$, i.e. the total number of cycles of the length $s = \{1, \dots, N\}$ in a graph with the adjacency matrix \mathbf{A} , [27]. While interesting in the number of cycles X_s^0 in the random graph $\mathbb{G}(N, k)$, we note that, in the matrix \mathbb{A} , for each entry proportional to r contributing in a cycle there is always the entry $1/r$ presented such that they are divided out. Therefore, one can prove that $\text{Tr}(\mathbb{A}^s) = \text{Tr}(\mathbf{A}^s) = X_s^0$. We recall that $X_1^0 = 0$ is the number of loops which are ruled out in our model.

Collecting the results of the present subsection and taking the expression (19) for the mean turbulent fraction $\langle F \rangle$ together with its formal definition (3) into account, we arrive at the equation for the free energy \mathcal{U} of the randomly coupled CM map system,

$$\mathcal{U} = \log(1 - \varepsilon) + \lambda_0 \frac{\partial \log Z}{\partial r} - \frac{1}{N} \sum_{s>1}^N \frac{1}{s} \left[\frac{\varepsilon}{k(1 - \varepsilon)} \right]^s X_s^0, \quad (23)$$

where Z is the partition function (17).

The first term in the Eq. (23) is irrelevant to either the coupled maps dynamics or the random network topology. The second one is a cumulative contribution from all chaotic configurations

allowed $\eta \in M_{\Phi, \mathbb{G}}^s$ which coincide with a given one on the cylinder \mathbb{L} . Finally, the third term represents a contribution from the topology of random network.

The Eq. (23) can hardly be solved explicitly. Nevertheless, some extremal solutions of (23) can be found easily.

6.2 Transitions to the spatio-temporal intermittency and relaminarization

Transitions to the spatio-temporal intermittency and relaminarization deserved the name of phase transitions since the behavior of the mean turbulent fraction $\langle F \rangle$ close to the "critical" values of coupling ε_c very resembles the behavior of thermodynamical quantities close to a critical point.

For the connectivity $k = 2$, the coupled maps defined on either regular lattice, [4], or at random exhibit a scaling behavior $\langle F \rangle \propto (\varepsilon - \varepsilon_c)^\beta$ with some critical exponent β that is typical for a second order phase transition. In contrast, the transition between laminar states and turbulence for either the RCMN with $k \geq 3$ or the globally coupled maps, [22], appears as a discontinuous jump in $\langle F \rangle$, a feature associated to a first order phase transitions.

For a backward transition from turbulence to a uniformly laminar states, the situation is different. For minimal connectivities, in both regular coupled maps with local interactions [4] and randomly coupled maps, such a transition does not occur for any $\varepsilon < 1$. For either globally coupled maps, [22], or randomly coupled maps with connectivities around $k = 10$, this transition appears as a discontinuous jump. However, for randomly coupled maps with connectivities $k > 10$, this transition meets a power law behavior in $\langle F \rangle$ with another critical exponent γ . Data show convincingly that the formal analogy with phase transitions occurring in statistical mechanics cannot provide us the complete and adequate classification for "critical" phenomena in the RCMN.

It is quite obvious that in a laminar domain \mathcal{L} of the space of external parameters $\mathbb{D} \equiv \{\varepsilon, k, r\}$ the probability $P(\xi)$ (15) to observe a symbolic chaotic configuration ξ on \mathcal{L} is always $P = 0$ for any ξ . Therefore, one could expect that the potential (16) over the laminar domain \mathcal{L} is $\mathcal{F}|_{\mathcal{L}} = -\infty$.

When the coupling is small $\varepsilon \ll 1$, the influence of random graph topology is vanishing. Therefore, the series term in the r.h.s. of Eq. (23), in this case, can be neglected. Since $\mathcal{F} = \mathbb{V}\mathcal{U}$ and the cylinder volume \mathbb{V} is taken to be infinite, one can see that the Gibbs potential $\mathcal{F} = -\infty$ until

$$\langle F \rangle_{\min} < \frac{|\log(1 - \varepsilon_c)|}{\log r}. \quad (24)$$

This expression relates the minimal mean turbulent fraction $\langle F \rangle_{\min}$ which can arise at the onset of intermittency for a given value ε_c .

For ε that is not small, the random topology of the network becomes significant. Instead

(24), one obtains

$$\langle F \rangle_{\min} < \frac{|\log(1 - \varepsilon_c)|}{\log r} + \frac{1}{N \log r} \left| \sum_{s>1}^N \frac{1}{s^2} \left[\frac{\varepsilon_c}{1 - \varepsilon_c} \right]^s \right|. \quad (25)$$

Let us consider the series term in Eq. (23). In a random graph $\mathbb{G}(N, k)$, the numbers of cycles X_s^0 are the Poisson distributed random variables $\text{Po}(\lambda_s^0)$ with the means $\lambda_s^0 = k^s/s$. If the number of vertices N in the graph is very large, one can replace X_s^0 in (23) with their expectations λ_s^0 . Consequently, for N large, one arrives at the following expression

$$\begin{aligned} \frac{1}{N} \sum_{s>1}^N \frac{1}{s^2} \left[\frac{\varepsilon}{1 - \varepsilon} \right]^s &= \frac{\varepsilon^2}{4N(1 - \varepsilon)^2} \cdot F \left([1, 2, 2], [3, 3], \frac{\varepsilon}{1 - \varepsilon} \right) \\ &\quad - \frac{\varepsilon^{N+1}}{N(N+1)^2(1 - \varepsilon)^{N+1}} \cdot F \left([1, N+1, N+1], [2+N, 2+N], \frac{\varepsilon}{1 - \varepsilon} \right) \end{aligned} \quad (26)$$

where $F([a], [b], x)$ is the generalized hypergeometric function, in which $[a]$ and $[b]$ are the sets of parameters.

The behavior of the term (26) in ε strongly depends of the random graph topology at given k . For random graphs with minimal connectivities $k = 2$, the random variables counting the number of small cycles which length s exceeds some maximal length $s > s_{\max}$ is $X_s^0 = 0$. s_{\max} cannot exceed the size of the giant component of the random graph $\mathbb{G}(N, k)$ but, actually, it is much less. Hence, the effective summation in the r.h.s. of Eqs. (23) and (25) is up to $s_{\max} \ll N$. The contribution to (23) coming from the term (26) slowly increases with ε as $\varepsilon < 1/2$ enhancing the critical value ε_c of the intermittency onset.

The series term (26) plays the crucial role in the transition to a uniformly laminar state. As $k \gg 1$ and $\varepsilon/(1 - \varepsilon) \gg 1$, the value of the sum abruptly jumps at some value $\varepsilon > 1/2$ to numbers much larger than N . Herewith, the major contribution to the sum comes from the Hamilton cycles $s = N$. The window of turbulence is closed when $\mathcal{U} < 0$.

We conclude this subsection with a notion of that there is no any turbulent window would appear in the system as $k \geq 100$. In previous sections, we have shown that for connectivity values $k \gg 1$, the relevant random graph $\mathbb{G}(N, k)$ has no isolated vertices, i.e. for every ordered pair of vertices ω_i and ω_j there is a path in $\mathbb{G}(N, k)$ starting in ω_i and terminating at ω_j . Following a traditional terminology, we shall call such a graph as *irreducible*. Consequently, the adjacency matrix A of the irreducible graph purports to meet the following property: for each pair of indices (i, j) there exists some $n \geq 0$ such that $A_{ij}^n > 0$, [27]. The typical length of the shortest path between two arbitrary vertices in an irreducible random graph is $d_{\omega_i \omega_j} = \log N / \log k$, [32].

Let us consider the adjacency matrix A of the graph irreducible $\mathbb{G}(N, k)$. Define a *period* p_ω of a node $\omega \in \Omega$ as the greatest common divisor of those integers $n \in \mathbb{N}$ for which $(A^n)_{\omega\omega} > 0$. Then the period p_A of the matrix is the greatest common divisor of the numbers p_ω , $\omega \in \Omega$, [27].

It is to be noticed that in the model in question $p_A = 2$, since loops are ruled out. We shall call the nodes ω_i and ω_j as *period equivalent*, if the length of path between them, $d_{\omega_i \omega_j}$

is divisible by p_A . One can see that as $k = 100$, for $N = 10^4$, all the nodes of the network are period equivalent and, therefore, synchronized.

6.3 Transitions to the collective behavior in RCMN

Within windows of turbulence, the Gibbs states given by the formula (15) is not trivial, and the Gibbs potential \mathcal{F} remains finite. A phase transition to the collective behavior occurs in the system of coupled maps, in thermodynamic limit $N \rightarrow \infty$, when the Gibbs state (15) is not unique, i.e. there are several (at least two) different Gibbs states with respect to the potential \mathcal{F} defined on symbolic configurations in M_{Φ}^s .

In the context of thermodynamic formalism applied to CML, this idea has been pronounced in [17]. For each topologically mixing component of the uniformly hyperbolic subset $K \subseteq M_{\Phi, \mathbb{G}}^s$, there is precisely one asymptotic probability distribution which is called the SRB measure (after Sinai-Ruelle-Bowen) on the attractor. For n -periodic components of K , however, there are n different Gibbs states relevant to n -cycling through the subcomponents.

In this subsection, we demonstrate that, in the thermodynamic limit $N \rightarrow \infty$, the Gibbs potential and consequently the free energy function are multivalued functions as $\varepsilon > 1/2$.

Let us compute the sum in the r.h.s. of the Eq. (23) as $N \rightarrow \infty$. In this case, one obtains

$$\lim_{N \rightarrow \infty} \sum_{s=1}^N \frac{1}{s} \left[\frac{\varepsilon}{k(1-\varepsilon)} \right]^s X_s^0 = \text{Polylog} \left(2, \frac{\varepsilon}{1-\varepsilon} \right) - \frac{\varepsilon}{1-\varepsilon} \quad (27)$$

where $\text{Polylog}(2, \alpha)$ is the polylogarithm function.

The point $\varepsilon = 1/2$ is a branch point for all branches of the polylogarithm function. The branch cut can be taken to be the interval $(1, \infty)$. The point $\varepsilon = 0$ is also a branch point, and the branch cut is taken to be the negative real axis. For the branches other than the principal branch which is given on the unit disk by the series

$$\text{Polylog}(2, \alpha) = \sum_{k=1}^{\infty} \frac{\alpha^k}{k^2},$$

there is the general formula for the (n, m) -th branch of $\text{Polylog}(2, \alpha)$,

$$\text{Polylog}(2, \alpha) + 2i\pi n \log(\alpha) - 4\pi^2 nm, \quad n, m \in \mathbb{Z}$$

where $\log(\alpha)$ means the principal branch of the logarithm [34].

If we now introduce the result (27) into Eq. (23) and then neglect terms $O(1/N)$ as $N \rightarrow \infty$, we arrive at the expression

$$\mathcal{U}_{y, m} = \log(1 - \varepsilon) + \lambda_0 \frac{\partial \log Z}{\partial r} - 4\pi^2 y m - 2\pi y i \log \left(\frac{\varepsilon}{1-\varepsilon} \right) + O \left(\frac{1}{N} \right). \quad (28)$$

which reveals the two-parameters set of branches for the free energy function \mathcal{U} . Here, we have introduced $m \in \mathbb{Z}$, and $y \equiv n/N \in \mathbb{R}$ as $N \rightarrow \infty$. The discrete parameter m enumerates different bands of possible solutions of the Eq. (23), and the parameter y (continuous in the thermodynamic limit) enumerates the different branches of \mathcal{U} within a band. The behavior prescribed by the Eq. (28) is clearly seen on the Figs. (9) and (10).

6.4 The bifurcation route to collective periodic behavior in RCMN

The graphs presented on the Figs. (9) and (10) essentially resemble the "bifurcation diagrams" well known in deterministic chaotic dynamics of the unimodular polynomial maps over the interval $I = [0, 1]$ having a negative Schwarzian derivative.

Consider the irreducible random graph $\mathbb{G}(N, k)$ and denote its adjacency matrix as A . The Perron-Frobenius theory is applied completely to such an irreducible matrix. As a particular consequence of this theory concerning the collective behavior in the RCMN, one proves that there exist two stable fixed points for the map $\Psi : F_t \rightarrow F_{t+1}$ correspondent to either the uniformly synchronized laminar state or the sustained fully turbulent state of network. Close to these fixed points, a map for the instantaneous turbulent fraction Ψ is a polynomial map in F_t . Therefore, in the unite interval $I = [0, 1]$ it turns to be a unimodal function having the negative Schwarzian derivative over the whole interval,

$$\mathcal{S}\Psi \equiv \frac{\Psi'''}{\Psi'} - \frac{3}{2} \left(\frac{\Psi''}{\Psi'} \right)^2 < 0. \quad (29)$$

In this case, Ψ displays an infinite sequence of pitchfork bifurcations when the attractor relevant to the unique Gibbs state losses its stability. An example of such a map have been presented in [22]. These bifurcations are really observable in some intervals of the parameter values.

In the diagrams shown on Figs. 9 and 10, the bifurcation branches which draw away from the stable point $F_t = 1$ terminate soon, while for the branches which tend to the fixed point where the map Ψ is still polynomial, the consequent pitchfork bifurcations are still observable up to the very end of the turbulent window.

7 Conclusion

In this paper we have studied some features associated with transitions to the spatio-temporal intermittency and relaminarization as well as transitions to the collective behavior occurring in the randomly coupled Chaté-Manneville "minimal" maps. We have reviewed and classified the previous studies devoted to randomly coupled maps networks according to the random graphs spanning the entire random network. We have studied the probabilistic geometrical properties of the k -out model random graphs $\mathbb{G}(N, k)$. The thermodynamic formalism based on the symbolic representation for the dynamics of randomly coupled chaotic maps has been introduced.

We have considered the Gibbs potential and free energy function for the system of randomly coupled maps and derive a closed equation for them. Some properties of solutions for this equation have been analysed. In particular, it has been proved that in some interval of external parameters (i.e., coupling, connectivity, and the governing parameter of the Chaté-Manneville map) the Gibbs potential together with the free energy function acquires the two-parameters set of branches. The non-uniqueness of the Gibbs state with respect to the given potential reveals itself in a complex collective periodic behavior.

We have found that in dependence of the connectivity value the onset of turbulence in the randomly coupled chaotic maps can occur as either a power law or a discontinuous jump of the instantaneous turbulent fraction F_t close to the critical value of coupling ε_c . Previous studies of the coupled Chaté-Manneville maps defined on the regular lattices have shown that F_t exhibits the scaling behavior close to the critical coupling for systems with local (diffusive) coupling and demonstrates a discontinuous jump for the globally coupled systems.

As connectivity grows up, a synchronization of the system to a uniformly laminar state would occur at some another critical value of coupling $\varepsilon'_c > \varepsilon$. Similar to the case of globally coupled maps, the windows of turbulence are established. Herewith, the onset of relaminarization process appears as a discontinuous jump to a uniformly laminar state if the connectivity is around $k = 10$, and as a power law decay of the mean turbulent fraction $\langle F \rangle$ close to ε'_c for $k > 10$. Randomly coupled chaotic maps systems of higher connectivities $k \geq 100$ are free of turbulence.

8 Acknowledgements

The authors are grateful to the participants of seminars in the Zentrum für Interdisziplinäre Forschung, Universität Bielefeld, especially to R. Lima and A. Pikovsky for illuminating discussions. S.S. is grateful to Prof. Dr. M. G. Cosenza for introduction to the problem and useful suggestions during numerical simulations. This work has been performed in connection to the international research project "The Sciences of Complexity: From Mathematics to technology to a Sustainable World", Zentrum für Interdisziplinäre Forschung (ZIF), Universität Bielefeld. One of the authors (D.V.) has been supported by the Alexander von Humboldt Foundation (Germany).

References

- [1] K. Kaneko, Progr. Theor. Phys. **72** 480 (1984); **74** 1033 (1985).
- [2] K. Kaneko, Physica D **23**, 436-447 (1986).
- [3] K. Kaneko, Physica D **41**, 137 (1990).
- [4] H. Chaté, P. Manneville, Chaos **2**, 307 (1992).
- [5] S. C. Manrubia, A. S. Mikhailov, EPrint arXiv: Mutual Synchronization and Clustering in Randomly Coupled Chaotic Dynamical Networks, cond-mat/9905083 (1999).
- [6] H. Chaté, P. Manneville, Physica D **32**, 409 (1988).
- [7] P. Erdős and A. Rényi, Publicationes Mathematicae **6**, 290 (1959).
- [8] B. Bollobás, *Random Graphs*, Academic Press, NY (1985).

- [9] S. Janson, T. Łuszak, A. Rucinski, *Random Graphs*, John Wiley & Sons, NY (2000).
- [10] M. G. Cosenza, R. Kapral, Phys. Rev. A **46**, 1850 (1992).
- [11] P.M. Gade, H. A. Cerdeira, Phys. Rev. E **52**, 2478 (1995).
- [12] S. Wasserman, K. Faust, *Social Network Analysis*, Cambridge Univ. Press, Cambridge (1994).
- [13] R. T. Paine, Nature **355**, 73 (1992), K. McCann, A. Hastings, and G. R. Huxel, Nature **395**, 794 (1998).
- [14] R. Albert, H. Jeong, and A.-L. Barabási, Nature **401**, 130 (1999), B. A Huberman, L. A. Adamic, Nature **401**, 131 (1999).
- [15] P. Grassberger, T. Schreiber, Physica D **50**, 177 (1991).
- [16] J. M. Houlrik, I. Webman, M. H. Jensen, Phys. Rev. A **41**, 4210 (1990).
- [17] G. Gielis, R. S. MacKay, Nonlinearity, **13**, 867 (2000).
- [18] Sinai Ya., Russ. Math. Surveys **28**, 21 (1972)
- [19] D. Ruelle, *Thermodynamic Formalism*, **5** of *Encyclopedia of Mathematics and its Applications* (Addison-Wesley, Reading, Mass., 1978)
- [20] M. Jiang, private communications. D.V. is grateful to M. jiang for this comment.
- [21] H. Chaté, Physica D **86**, 238 (1995).
- [22] M.G. Cosenza, A. Parravano, Phys. Rev. E **53**, 6032 (1995).
- [23] M. G. Cosenza, R. Kapral, Chaos **4**, 99 (1994).
- [24] P. Gade, Phys. Rev. E **54**, 64 (1996).
- [25] V. F. Kolchin, *Random Mappings*, Optimization Software, NY (1986).
- [26] D. J. Aldous, J. Pitman, Random Structures Algorithms **5**, 487 (1994).
- [27] D. Lind, B. Marcus, *An Introduction to Symbolic Dynamics and Coding*, Cambridge Univ. Press., Cambridge (1995).
- [28] S. Janson, Combin. Probab. Comput. **4**, 369 (1995).
- [29] J. Bricmont, A. Kupiainen, Commun. Math. Phys. **178**, 703 (1996).
- [30] M. Jiang, Ya. B. Pesin, Commun. Math. Phys. **193**, 1391 (1998).
- [31] The falling factorial is

$$(N)_m = N^m \exp \left(-\frac{m^2}{2N} - \frac{m^3}{6N^2} - O \left(\frac{m}{N} + \frac{m^4}{N^3} \right) \right) \sim N^m,$$

as $N \rightarrow \infty$.

- [32] M. E. J. Newman, S. H. Strogatz, and D. J. Watts, EPrint arXiv: Random graphs with arbitrary degree distribution and their applications, cond-mat/0007235 (2000).
- [33] P. Erdős, A. Rényi, Publ. Math. Inst. Hungar. Acad. Sci. **5**, 17 (1960).
- [34] L. Lewin, *Polylogarithms and Associated Functions*, North Holland, Amsterdam (1981).
- [35] E. Friedgut, *Sharp Thresholds of Graph Properties, and the k -sat problem*, J. Amer. Math. Soc. **12**, 1017-1054 (1999).

9 Figures and Graphs

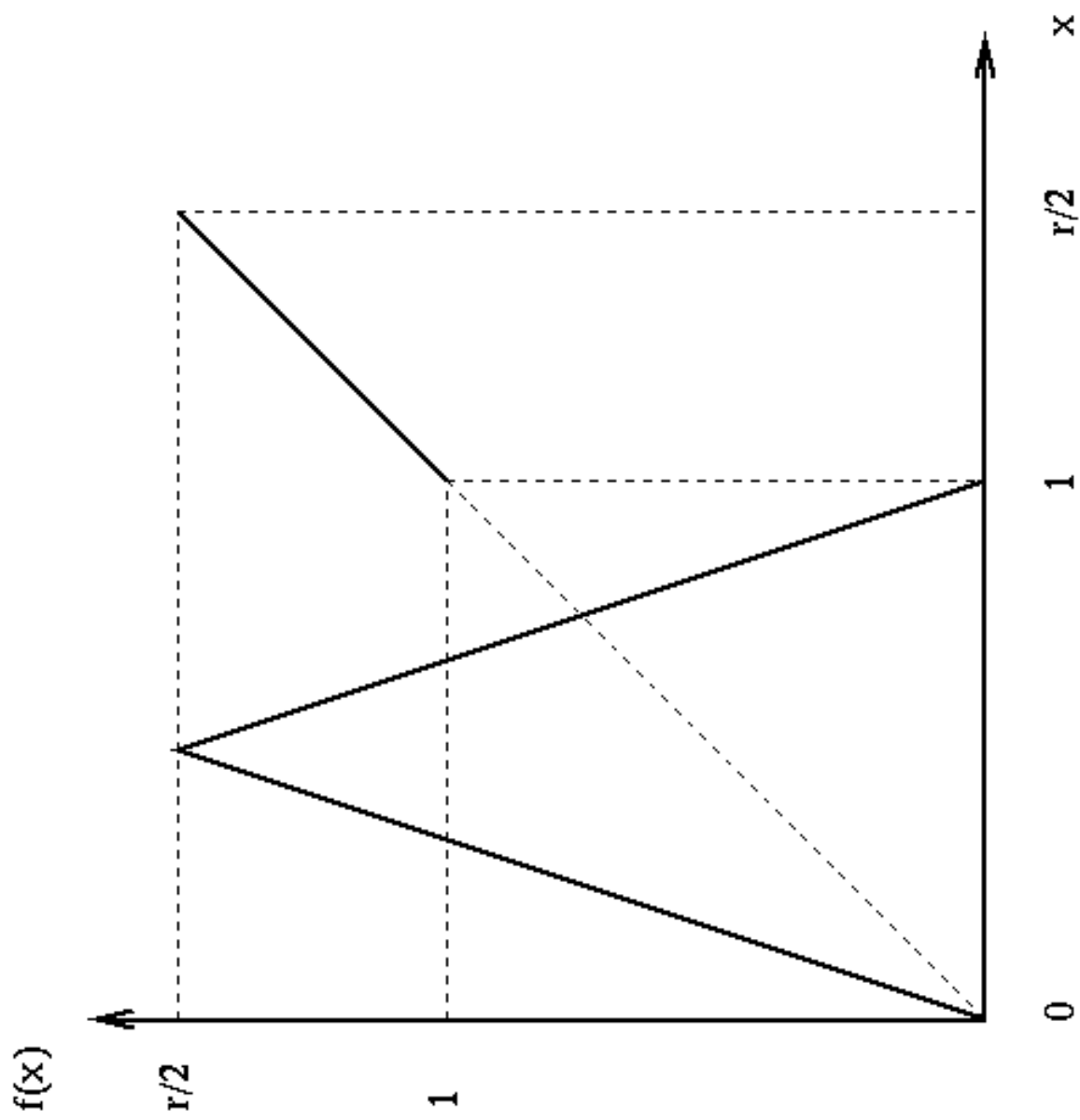


Figure 1: The Chaté-Manneville map for $r = 3.0$.

